Neurobiology of Aging xxx (2014) 1–10

Contents lists available at ScienceDirect

Neurobiology of Aging

journal homepage: www.elsevier.com/locate/neuaging

White matter changes in preclinical Alzheimer's disease: a magnetic resonance imaging-diffusion tensor imaging study on cognitively normal older people with positive amyloid β protein 42 levels

José Luis Molinuevo [a,b], Pablo Ripolles [c,d], Marta Simó [c], Albert Lladó [a,b], Jaume Olives [a,b], Mircea Balasa [a,b], Anna Antonell [a,b], Antoni Rodriguez-Fornells [c,d,e], Lorena Rami [a,b,*]

[a] Alzheimer's Disease and Other Cognitive Disorders Unit, Neurology Service, Hospital Clínic, Barcelona, Spain
[b] Institut d'Investigacions Biomèdiques August Pi i Sunyer (IDIBAPS), Barcelona, Spain
[c] Cognition and Brain Plasticity Group, Bellvitge Biomedical Research Institute- IDIBELL, L'Hospitalet de Llobregat, Barcelona, Spain
[d] Department of Basic Psychology, Campus Bellvitge, University of Barcelona, L'Hospitalet de Llobregat, Barcelona, Spain
[e] Institució Catalana de Recerca i Estudis Avançats, ICREA, Barcelona, Spain

ARTICLE INFO

Article history:
Received 21 January 2014
Received in revised form 28 May 2014
Accepted 31 May 2014

Keywords:
Alzheimer's disease
Diffusion tensor imaging
Cerebrospinal fluid
Cognition
Diagnosis
Preclinical phases

ABSTRACT

The aim of this study was to use diffusion tensor imaging measures to determine the existence of white matter microstructural differences in the preclinical phases of Alzheimer's disease, assessing cognitively normal older individuals with positive amyloid β protein (Aβ42) levels (CN_Aβ42+) on the basis of normal cognition and cerebrospinal fluid $A\beta_{42}$ levels below 500 pg/mL. Nineteen CN_Aβ42+ and 19 subjects with $A\beta_{42}$ levels above 500 pg/mL (CN_Aβ42−) were included. We encountered increases in axial diffusivity (AxD) in CN_Aβ42+ relative to CN_Aβ42− in the corpus callosum, corona radiata, internal capsule, and superior longitudinal fasciculus bilaterally, and also in the left fornix, left uncinate fasciculus, and left inferior fronto-occipital fasciculus. However, no differences were found in other diffusion tensor imaging indexes. Cognitive reserve scores were positively associated with AxD exclusively in the CN_Aβ42+ group. The finding of AxD alteration together with preserved fractional anisotropy, mean diffusivity, and radial diffusivity indexes in the CN_Aβ42+ group may indicate that, subtle axonal changes may be happening in the preclinical phases of Alzheimer's disease, whereas white matter integrity is still widely preserved.

1. Introduction

Disease-modifying therapies for Alzheimer's disease (AD) require intervention before the onset of dementia, and preventive therapies require intervention even before the clinical manifestation of AD symptoms. Great efforts have been made to identify asymptomatic at risk individuals who are likely to develop the disease. The neuropathologic burden of AD emerges very early during the course of the disease, preceding the appearance of clinical symptoms by more than 15 years (Iacono et al., 2008; Jack et al., 2010; Villemagne et al., 2013). In this regard, biomarkers, particularly amyloid markers, precede cognitive decline and can potentially aid early intervention and diagnosis (Jack et al., 2010; Villemagne et al., 2013). Cognitively normal subjects with a positive amyloid biomarker (CN_Aβ42+) which potentially are in the preclinical phase in the disease (Dubois et al., 2010; Sperling et al., 2011), present distinct structural features such as left hippocampal atrophy and greater cortical thinning in parietal, temporal, and frontal regions compared with control subjects (Arenaza-Urquijo et al., 2013; Fortea et al., 2011), as well as greater activation of the precuneus and posterior cingulate cortex during visual memory encoding using functional magnetic resonance imaging (MRI) (Rami et al., 2012).

Today, there is an increasing interest in the study of brain microstructure and white matter (WM) fibers. Diffusion tensor imaging (DTI) reflects tissue microstructure and may be able to capture subtle WM pathway changes even before cognitive alterations become apparent. This means that it is potentially a sensitive marker of brain degeneration in CN_Aβ42+, associated to

* Corresponding author at: Alzheimer's Disease and Other Cognitive Disorders Unit, Neurology Service, Hospital Clínic, Villarroel 170. 08036, Barcelona, Spain. Tel.: +34 932275785; fax: +34 932275783.
E-mail address: lrami@clinic.ub.es (L. Rami).

0197-4580/$ – see front matter © 2014 Elsevier Inc. All rights reserved.
http://dx.doi.org/10.1016/j.neurobiolaging.2014.05.027

the preclinical phase of the disease. DTI techniques are based on the analysis of water molecule movement in both GM and WM, and therefore allow the study of cerebral WM microstructure. The DTI indices, fractional anisotropy, axial, mean, and radial diffusivity, have been shown to be useful for characterizing and interpreting WM changes (Acosta-Cabronero et al., 2010; Alexander et al., 2007), and therefore, can be used to study axonal and WM pathways along the AD continuum, including its preclinical stage. Published studies of mild cognitive impairment (MCI) and AD patients have revealed distinct regional impairments, including reduced fractional anisotropy (FA) in the WM underlying the parietal lobes and posterior cingulate or the WM around the parahippocampal gyrus and the thalamus (Acosta-Cabronero et al., 2010, 2012; Bosch et al., 2012; Fellgiebel et al., 2005; Medina et al., 2006). In addition, some studies have found impairment of the perforant pathway that connects the entorhinal cortex with the hippocampus, suggesting the disconnection of the limbic structures from multimodal association regions which also project to the entorhinal cortex, a finding which may explain some of the cognitive deficits that characterize AD (Acosta-Cabronero et al., 2010; Kalus et al., 2006). Furthermore, the study of different DTI indexes seems to be a promising tool to detect incipient WM changes in CN_Aβ42+ subjects (Bosch et al., 2012).

From a clinical perspective, DTI as well as cerebrospinal fluid (CSF) values significantly predicted cognitive decline and atrophy in the medial temporal lobe in subjects with subjective cognitive decline and MCI (Selnes et al., 2013). DTI indexes in white matter regions adjacent to brain structures affected early in AD have also been associated with high levels of total tau (t-tau) protein in healthy cognitive adults (Bendlin et al., 2012). Recently, a group of presymptomatic presenilin 1 mutation carriers showed reduced mean diffusivity in the right hippocampus and reduced mean and axial diffusivity in the right cingulum (Ryan et al., 2013). However, the degree of axonal injury present in CN_Aβ42+ has not been well established.

On the other hand, differences in the lag phase between CSF protein deposition, like Aβ42, and the appearance of symptoms may be partially caused by interindividual differences in brain reserve (Katzman, 1993) and/or cognitive reserve (CR) (Stern, 2009). Brain reserve refers to interindividual differences in the neural substrate, such as a greater synaptic density or a larger number of neurons to support normal function despite pathologic processes. Cognitive reserve is the capacity of the adult brain to cope with more advanced pathology by taking advantage of functional resources (e.g., the capacity to use alternative networks or cognitive strategies to cope with the effects of the pathology). Recently, our group found a significant relationship between decreased volume of the left hippocampus or decreased cortical thickness of the right supramarginal gyrus and higher scores on a cognitive reserve questionnaire in asymptomatic healthy elders with low Aβ42 CSF levels, hence termed CN_Aβ42+ (Arenaza-Urquijo et al., 2013). These results indicated that subjects with abnormal Aβ42 CSF levels, who may be at a higher risk of developing AD, and high scores on our cognitive reserve questionnaire, may be tolerating a more advanced neurodegenerative process in critical cortical and subcortical regions.

The aim of this study was to use DTI measures to determine WM differences in the preclinical phase of the disease, assessing normal cognitive subjects with CSF Aβ42 levels below 500 pg/mL (Dubois et al., 2010; Sperling et al., 2011), and to test the hypothesis that the preclinical state of AD is distinct from normal aging. We hypothesized that CN_Aβ42+ will present incipient degeneration of the WM pathways that connect posterior brain areas, with a similar pattern of WM changes as those reported in MCI and AD patients. An additional objective was to elucidate whether high scores on cognitive reserve questionnaire were also associated with WM changes, and thus, might aid CN_Aβ42+ subjects to tolerate a more advanced stage of WM degeneration.

2. Methods

2.1. Subjects

Thirty-eight subjects were recruited from the Alzheimer's disease and other cognitive disorders Unit of the Hospital Clinic, Barcelona, Spain. All accepted to participate in the project. All subjects underwent clinical and neuropsychological assessment, MRI, and lumbar puncture. The study was approved by the local ethics committee, and all participants gave written informed consent before enrollment.

Nineteen participants were classified as CN_Aβ42+. CN_Aβ42+ were defined, following Sperling et al. (2011) recommendations, as: (1) objective cognitive performance in all tests from a specific neuropsychological battery (see the following) within the normal range (performance within 1.5 standard deviation [SD]); (2) no significant psychiatric symptoms or previous neurological disease; (3) the absence of dementia or significant functionally impairment; and (4) decreased CSF Aβ42 (<500 pg/mL) levels. Because WM changes may be very sensitive to aging, we decided a priori to perform a matched age, level of education and gender study. Therefore, nineteen cognitively normal older with negative Aβ42 levels (CN_Aβ42−) were selected to match the CN_Aβ42+ group in age, level of education and gender. Normal cognitive CN_Aβ42− were defined as: (1) cognitive performance in all tests, from a specific neuropsychological battery (see the following), within the normal range (performance within 1.5 SD); (2) no significant psychiatric symptoms or previous neurologic disease; (3) the absence of functional impairment; and (4) normal Aβ42 levels (>500 pg/mL).

Twelve subjects from the CN_Aβ42− group and 10 from the CN_Aβ42+ group presented subjective cognitive complaints, although they scored within the normal range in all tests of the neuropsychological battery. Subjects with subjective cognitive complaints had attended the clinic for memory concerns but were found to have normal cognition. The rest of the subjects, in both groups, were normal cognitive spouses of patients attending the clinic or volunteers attending the clinic who were participating in scientific projects.

2.2. Determination of CSF biomarkers

Subjects underwent lumbar puncture between 9 AM and 12 PM. CSF (10 mL) was collected. The samples were centrifuged and stored in polypropylene tubes at −80 °C within the first hour after extraction. Levels of Aβ42, t-tau, and phosphorylated tau at threonine-181 (p-tau) were measured by enzyme-linked immunosorbent assay kits (Innogenetics, Ghent, Belgium). A cutoff point of 500 pg/mL was used to dichotomize the sample into Aβ42 positive (CN_Aβ42+) subjects, who had a CSF Aβ42 level <500 pg/mL, and Aβ42 negative subjects (CN_Aβ42−), who had a CSF Aβ42 level greater than 500pg/mL. The cutoff score was established in agreement with the internal values of our laboratory (Antonell et al., 2011).

2.3. Cognitive and functional assessment

Participants were administered a 1-hour neuropsychological battery test by a trained neuropsychologist. The battery included memory, language, praxis, visual perception, frontal functions assessment, and the Cognitive Reserve Questionnaire (Rami et al.,

2011). All neuropsychological scores were adjusted for age and educational level. Normative neuropsychological data and the neuropsychological battery have been described in detail elsewhere (Rami et al., 2007). A group of 19 subjects (8 CN_Aβ42+ and 11 CN_Aβ42−) underwent a follow-up cognitive examination. All participants were assessed 2 years after the first assessment (mean, SD: 24 months ± 1 month).

2.4. Scanning parameters

Data were collected on a 3T scanner (Siemens Magnetom Trio). The session started with the acquisition of a T1-weighted, high-resolution structural MRI (echo time [TE] = 2.98 ms, repetition time [TR] = 2300 ms, inversion time = 900 ms, flip angle = 9°, bandwidth = 240 Hz/pixel, matrix = 256 × 256, 240 axial slices, isometric voxel size = 1.0 mm^3). DTI-scans were acquired using a spin-echo EPI sequence with coverage of the whole head (60 axial slices, TR: 7600 ms, TE: 89 ms, acquisition matrix: 122 × 122 × 60, voxel size: 2.0 × 2.0 × 2.0 mm^3). Two runs with 1 non-diffusion weighted volume and 30 diffusion weighted volumes (b-values of 1000 s/mm^2) were acquired. An additional Fluid Attenuated Inversion Recovery (FLAIR) was also acquired (40 axial slices, TR: 9000 ms, TE: 96 ms, acquisition matrix: 228 × 256, voxel size: 0.9375 × 0.9375 × 3.3 mm^3). An 8-channel coil array using generalized autocalibrating partial parallel acquisition with 2-fold acceleration was used. Acquisition time was around 20 minutes (7 minutes 48 seconds for the T1, 4 minutes 23 seconds for each of the DTI runs and 2 minutes 44 seconds for the FLAIR).

2.5. Assessment of white matter hyperintensities

We qualitatively evaluated the presence of white matter hyperintensities on FLAIR images using a 4-point rating scale (Wahlund et al., 2001). This rating scale consists of: 0 for no lesions, 1 for focal lesions, 2 for beginning confluence of lesions, and 3 for diffuse involvement of the entire regions with or without involvement of U fibers.

2.6. DTI-MRI cognition analysis

Raw DTI-MRI data were analyzed using the FMRIB's Diffusion Toolbox, which is part of the FMRIB Software Library (FSL 5.0.1, www.fmrib.ox.ac.uk/fsl/; Jenkinson et al., 2012; Smith et al., 2004; Woolrich et al., 2009). The 2 runs acquired were first concatenated in a single file and then corrected for eddy current distortions and head motion using FMRIB's linear registration tool (Jenkinson and Smith, 2001). Subsequently, the gradient matrix was rotated to provide a more accurate estimate of diffusion tensor orientations (Leemans and Jones, 2009). Following this, brain extraction was performed using the Brain Extraction Tool (Smith, 2002), which is also part of the FSL distribution.

When the medium is anisotropic, as in white matter, water molecules diffuse in a particular direction, which can be modeled as an ellipsoid tensor (Basser et al., 1994a, 1994b). Therefore, the analysis continued with the reconstruction of the diffusion tensors using the linear least-squares algorithm included in the Diffusion Toolkit 0.6.2.2 (Ruopeng Wang, Van J. Wedeen, trackvis.org/dtk, Martinos Center for Biomedical Imaging, Massachusetts General Hospital). The tensor reconstructed at each voxel can be decomposed into 3 eigenvectors which describe the direction along each of the 3 axes. The corresponding eigenvalues can be considered as a measure of the diffusivity along each axis (λ_1 for the main direction; λ_2 and λ_3 for the other 2 directions) (Alexander et al., 2007). Mathematical combinations of the 3 eigenvalues can be used to compute several measures of anisotropy: axial diffusivity (AxD) is described as the diffusivity along the main direction (λ_1); radial diffusivity (RD) is computed as the average of the diffusivities along the 2 other directions $\left(\frac{\lambda_1+\lambda_2}{2}\right)$; the average of the 3 diffusivities yields the mean diffusivity (MD) $\left(\frac{\lambda_1+\lambda_2+\lambda_3}{3}\right)$; a combination of the 3 eigenvalues $\left(\sqrt{\frac{(\lambda_1-MD)^2+(\lambda_2-MD)^2+(\lambda_2-MD)^2}{2(\lambda_1+\lambda_2+\lambda_3)}}\right)$ is used to compute FA. All these measures have been previously used to assess white matter integrity in patients suffering from AD (Acosta-Cabronero et al., 2010, 2012; O'Dwyer et al., 2011). Therefore, FA, RD, AxD, and MD maps were calculated for each participant using the eigenvalues extracted from the diffusion tensors.

The registration of the participants' individual images to a common template, ensuring a one-to-one correspondence among the brain anatomies of all the individuals in the group, is of crucial importance in the second level MRI analyses. When applied to patients suffering from neurodegenerative diseases and brain insults, this process becomes more prone to misregistrations (Ripolles et al., 2012). To overcome this and other limitations, the Tract Based Spatial Statistics (TBSS; Smith et al., 2006) was developed. From each subject's normalized FA image, TBSS extracts the most relevant tract center, building a skeleton which contains the main tracts common to all participants in a study. In addition, TBSS has been successfully applied to AD (Acosta-Cabronero et al., 2010, 2012; O'Dwyer et al., 2011).

Voxel based analyses of FA, RD, AxD, and MD maps were performed using TBSS. FA maps from all participants were registered to the FMRIB58_FA 1 × 1 × 1 mm^3 template (MNI152 space) applying the nonlinear registration tool FNIRT (Andersson et al., 2007a, 2007b). All normalized FA maps were then averaged to create a mean FA volume, from which a mean FA skeleton, representing the centers of all tracts common to all participants in the study, was derived. Each participant's normalized FA data were projected onto this skeleton by searching for the highest FA value within a search space perpendicular to each voxel of the mean skeleton. This process was repeated for the RD, AxD, and MD maps, by applying the transformations previously calculated for the FA maps. In the end, 4 different sets of skeletons (FA, RD, AxD, and MD) for both CN_Aβ42− and CN_Aβ42+ groups were obtained.

Comparisons between groups in both directions (CN_Aβ42− > CN_Aβ42+ and CN_Aβ42+ > CN_Aβ42−) were carried out in a second level analysis, using all 4 different diffusion measures. As both groups were matched by age, gender, and years of education no nuisance covariates were added to the model. However, to ensure that the differences obtained could not be biased by age or gender, post hoc analysis comparing the groups and controlling for age and age plus gender were also calculated.

Moreover, to ensure that participants with subjective cognitive complaints were not biasing the study, 3 extra analyses were calculated. First, we recalculated the original analysis (19 CN_Aβ42+ vs. 19 CN_Aβ42−) adding the subjective cognitive complainer status as a variable of nuisance. Second, within the CN_Aβ42− group, a comparison between non-complainers (7 participants) and subjective complainers (12 participants) was carried out. We expected this comparison to yield no significant results, implying that all participants had a similar brain structure as measured by DTI-MRI. And third, we also computed group comparisons between CN_Aβ42+ and CN_Aβ42− subjective complainers (12 subjective cognitive complainers in the CN_Aβ42−

Table 1
Demographics, CSF biomarker levels, and neuropsychological performance of groups.

	CN_Aβ42+ (n = 19)	CN_Aβ42− (n = 19)	*t*-value; *p*-value
Age	69.94 ± 7.58	69.21 ± 5.61	$t(36) = 0.34$; >0.73
Years of education	10.26 ± 4.43	9.94 ± 4.00	$t(36) = 0.23$; >0.81
Gender (%women)	68.4 %	63.1	χ^2; >0.74
$A\beta_{42}$	359.12 ± 81.31	743.61 ± 162.58	$t(36) = -9.21$; <0.001[a]
p-tau	68.64 ± 43.43	70.85 ± 40.11	$t(36) = -0.16$; >0.87
t-tau	398.09 ± 439.04	395.85 ± 284.14	$t(36) = 0.01$; >0.98
CRQ	13.63 ± 5.74	14.42 ± 1.83	$t(36) = -0.45$; >0.64
FCSRT L	10.36 ± 2.63	10.42 ± 2.45	$t(36) = -0.06$; >0.94
FCSRT TL	11.57 ± 3.84	11.68 ± 3.41	$t(36) = -0.09$; >0.92
FCSRT R	10.73 ± 2.68	11.31 ± 2.28	$t(36) = -0.71$; >0.47
FCSRT TR	11.94 ± 3.86	12.52 ± 3.73	$t(36) = -0.46$; >0.64
CERAD_R	4.8 ± 1.82	5.61 ± 1.66	$t(36) = -1.23$; >0.22
M@T	44.11 ± 4.87	46.18 ± 3.0	$t(34) = 1.51$; >0.14
MMSE	27.79 ± 1.61	28.32 ± 1.41	$t(36) = 1.06$; >0.29
BNT	51.37 ± 4.47	52.26 ± 4.13	$t(36) = 0.64$; >0.52
VOSP_numbers	11.42 ± 4.84	11.78 ± 3.99	$t(36) = 0.71$; >0.48
TMT-A	55.74 ± 27.56	50.58 ± 19.25	$t(36) = -0.66$; >0.51
TMT-B	159.06 ± 99.61	129.79 ± 75.73	$t(34) = -1.0$; >0.32

Key: BNT, Boston naming test; CERAD R, CERAD memory_ recall; CRQ, Cognitive Reserve Questionnaire; CSF, cerebrospinal fluid; FCSRT, Free and Cued Selective Reminding Test; FCSRT L, learning; FCSRT TL, total learning; FCSRT TR, total recall; M@T, Memory Alteration Test; MMSE, Mini-Mental State Examination; TMT-A, Trail making test A; TMT-B, Trail making test B; VOSP_numbers, Visual Object and Space Perception Battery_number location task.
[a] $p < 0.001$.

group versus 10 complainers in the CN_Aβ42+ group). We hypothesized that this analysis was going to show a similar pattern of results, although at a lower threshold because of the reduced sample size (19 CN_Aβ42+ vs. 19 CN_Aβ42−), as the main analysis that included all subjects.

Unless otherwise noted, results are reported at an FWE-corrected $p < 0.05$ value using threshold-free cluster enhancement (Smith and Nichols, 2009) and a nonparametric permutation test with 5000 permutations (Nichols and Holmes, 2002).

A post hoc analysis was planned for the areas detected during group comparisons. For each participant and measure (FA, RD, AxD, or MD), all the skeleton voxels showing significant differences between groups were averaged to obtain one representative value per subject. Correlations between these values and each subject's cognitive measures (basal neuropsychological tests and Cognitive Reserve questionnaire) and CSF biomarker levels (Aβ42, t-tau, and p-tau) were performed. These correlations were calculated separately for each group. Cognitive changes were examined using repeated measures analyses of variance with group as a between-subjects factor and time (baseline, end of follow-up) as a within-subject factor. Pearson correlation coefficient was used to study the relation between AxD index and the cognitive change observed (change in test scores at follow-up).

3. Results

3.1. Demographic, clinical, and CSF characteristics

Demographic and clinical characteristics are summarized in Table 1. There were no differences in age, gender, or years of education between CN_Aβ42− and CN_Aβ42+. As expected, the level of Aβ42 was significantly lower in CN_Aβ42+ than in CN_Aβ42−. There were no differences in t-tau and p-tau levels, nor there were differences in APOE status between groups ($p > 0.05$).

3.2. Basal and follow-up neuropsychological data

As far as neuropsychological features were concerned, there were no significant differences between groups on any cognitive test, including the Cognitive Reserve questionnaire for the basal

Table 2
Basal and follow-up neuropsychological scores.

	CN_Aβ42− (n = 11) Mean (SD) (mean age: 69.21)		CN_Aβ42+ (n = 8) Mean (SD) (mean age: 69.95)	
	Basal	Follow-up 2 y	Basal	Follow-up 2 y
M@T	45.91 (3.20)	46.63 (2.33)	42.63 (7.02)	43.12 (6.05)
MMSE	28.08 (1.73)	27.83 (2.36)	27.60 (1.64)	27.00 (2.10)
FCSRT L	23.75 (5.02)	26.25 (6.03)	21.60 (8.20)	21.20 (10.95)
FCSRT TL	42.42 (5.33)	44.66 (3.57)	39.40 (7.39)	36.40 (11.01)
FCSRT R	9.58 (1.56)	9.75 (3.04)	8.50 (3.77)	6.80 (5.11)
FCSRT TR	14.67 (1.30)	14.58 (1.72)	13.30 (2.86)	12.00 (3.88)
CERAD_R	6.11 (1.36)	5.88 (2.93)	4.40 (2.51)	3.80 (3.11)
BNT	51.58 (4.64)	53.08 (5.35)[a]	52.33 (4.03)	49.88 (5.88)[a]
VOSP_numbers	8.67 (1.23)	10.08 (3.26)	8.67 (1.58)	9.33 (1.00)
TMT-A	55.08 (18.88)	51.50 (17.71)	49.60 (12.59)	47.70 (16.32)
TMT-B	157.25 (79.79)	132.00 (36.04)	135.13 (78.61)	125.37 (51.32)

Key: BNT, Boston naming test; CERAD R, CERAD memory_ recall; CRQ, Cognitive Reserve Questionnaire; FCSRT, Free and Cued Selective Reminding Test; FCSRT L, learning; FCSRT TL, total learning; FCSRT TR, total recall; M@T, Memory Alteration Test; MMSE, Mini-Mental State Examination; TMT-A, Trail making test A; TMT-B, Trail making test B; VOSP_numbers, Visual Object and Space Perception Battery_number location task.
[a] Significant differences, $p < 0.05$.

Table 3
Main differences in AxD between CN_Aβ42+ and CTR groups. Summary of local maxima differences for the CN_Aβ42+ > CTR contrast (CN_Aβ42+ have higher AxD than CN_Aβ42−). Results are shown at an FWE-corrected $p < 0.05$ value using threshold-free cluster enhancement and a nonparametric permutation test with 5000 permutations. MNI coordinates are used.

Axial diffusivity	Coordinates
Left superior corona radiata	−25, 7, 20[a]
Left posterior limb of the internal capsule	−21, −8, 18[a]
Left anterior limb of the internal capsule	−22, 9, 18[a]
Splenium of the corpus callosum	2, −29, 22[b]
Left external capsule	−31, 0, 13[b]
Right superior corona radiata	26, −17, 26[b]
Left superior longitudinal fasciculus	−44, −16, 28[b]
Left uncinate fasciculus	−23, 23, −3[b]
Right genu of the corpus callosum	−11, 28, 13[c]
Body of the corpus callosum	−2, −9, 26[c]
Right posterior limb of the internal capsule	25, −14, 15[c]
Right anterior limb of the internal capsule	17, 3, 10[c]
Right superior longitudinal fasciculus	38, −27, 32[c]
Left fornix	−27, −23, −5[c]
Left fronto-occipital fasciculus	−33, −29, 3[c]

Key: AxD, axial diffusivity.
[a] $p < 0.005$.
[b] $p < 0.01$.
[c] $p \leq 0.05$.

examination (Table 1). Table 2 shows basal and follow-up data of the 19 subjects (8 CN_Aβ42+ and 11 CN_Aβ42−) that could be studied after 2 years. Five subjects of the 8 CN_Aβ42+group, who also presented subjective complaints developed cognitive impairment during follow-up (2 years). Three of them developed memory impairment, fulfilling amnestic MCI criteria, and 2 of them developed memory, language, and perception cognitive problems, as well as functional impairment and they fulfilled criteria for probable AD. CN_Aβ42+ subjects presented significant language decline over time. Repeated measures ANOVA analysis showed a significant interaction between the factors of group and time of follow-up on Boston naming test ($F = 7.2$; $p > 0.015$). No other cognitive changes were detected in either group.

3.3. Assessment of white matter hyperintensities

FLAIR sequence was available in 13 of 19 preclinical subjects and in 14 of 19 healthy subjects. The median rating scale score was 1 (0–3) for preclinical subjects and 1 (0–2) for CN_Aβ42− subjects. No differences were found between rating scales (Mann-Whitney *U*-test; $p > 0.76$).

3.4. DTI-MR voxel based analysis

No differences between CN_Aβ42+ and CN_Aβ42− were found in FA, RD, or MD in any direction tested (CN_Aβ42− > CN_Aβ42+ or CN_Aβ42+> CN_Aβ42−). However, CN_Aβ42+ subjects showed increased AxD in the corpus callosum (splenium, body, and genu) corona radiata, internal capsule, and superior longitudinal fasciculus (SLF) bilaterally and also in the left fornix, left uncinate fasciculus, and left inferior fronto-occipital fasciculus (IFOF; see Table 3). We also performed additional analysis correcting for age and gender, which did not alter the results. These differences are shown in Fig. 1A over the FMRIB58_FA template, for better visualization of the white matter pathways. The same results (increased AxD in CN_Aβ42+ compared with CN_Aβ42−) are shown in Fig. 1B using a canonical T1-weighted template for improved localization of subcortical structures. In addition, templates for hippocampus, thalamus, and posterior cingulate (extracted from the WFU PickAtlas toolbox; Maldjian et al., 2003, 2004) are also shown in this figure.

Post hoc analysis controlling for age (Supplementary Fig. 1, first row) and age plus gender (Supplementary Fig. 1, second row) showed the same pattern of differences (increased AxD for CN_Aβ42+; no differences in MD, RD, or FA).

The extra analysis controlling for subjective cognitive complainer status also found the same pattern of results (again, increased AxD for CN_Aβ42+; no differences in MD, RD, or FA; Supplementary Fig. 1, third row). Moreover, the analysis comparing the 12 CN_Aβ42− with subjective complaints versus the 7 CN_Aβ42− without subjective complaints found no differences between subgroups neither in MD, AxD, RD, or FA, not even at a $p <$ 0.05 uncorrected threshold. This implies that both subgroups of CN_Aβ42− subjects have a similar brain structure as measured by DTI-MRI. Finally, the results from the comparison between the 12 CN_Aβ42− subjective cognitive complainers versus the 10 complainers in the CN_Aβ42+ group, once again showed the same pattern of results in the same brain areas (increased AxD for CN_Aβ42+; no differences in MD, RD, or FA; see Supplementary Fig. 1, fourth row). However, in this case, AxD showed differences between both groups at a $p < 0.01$ uncorrected for multiple comparisons threshold (the pattern of AxD abnormalities previously reported starts to appear at an FWE-corrected $p < 0.08$ threshold). This was probably because of the fact that we reduced the sample size (12 vs. 10 in the present analysis compared with 19 vs. 19 in the original analysis), thus losing statistical power. These additional analyses provide reassurance that the presence of subjective cognitive complaints in some individuals in the CN_Aβ42+ group is not a major source of bias in our results.

In addition, the cognitive reserve questionnaire score was positively correlated with AxD increases only for the CN_Aβ42+ ($r = 0.572$, $p < 0.013$; Fig. 2). Interestingly, no correlation was found for the CN_Aβ42− group ($r = 0.12$, $p > 0.62$); nor did we find significant correlations between AxD and Aβ42, tau, p-tau levels, or any other neuropsychological test.

3.5. AxD index and cognitive evolution

Subjects with higher AxD total levels showed higher memory deterioration after the 2 years follow-up in the whole group, as a significant correlation was found between basal AxD in the areas showing differences between groups and changes in scores in the Memory Alteration test (M@T) ($r = -0.47$; $p < 0.04$). No other correlations were found between changes in memory or other cognitive tests after the 2 years follow-up and basal AxD score. Fig. 3 shows the relationship between changes in memory scores (M@T) and AxD values in the subset of subjects who had longitudinal follow-up.

4. Discussion

The main finding of this study is that cognitively normal older people who have reduced CSF Aβ42 levels, indicating that they are at risk of developing AD, presented early differences in WM which can be detected by means of DTI-MRI imaging. We found increased AxD in CN_Aβ42+ relative to CN_Aβ42− in several WM regions: bilaterally in the corpus callosum, corona radiata, internal capsule, and SLF, and also in the left fornix, left uncinate fasciculus, and left IFOF. Cognitive reserve scores were only positively correlated with AxD values in CN_Aβ42+, suggesting that CR measures present an association with brain structure at this stage of the disease. In that sense, following the CR hypothesis, higher CR might have an influence in delaying cognitive symptoms in subjects already at risk for AD.

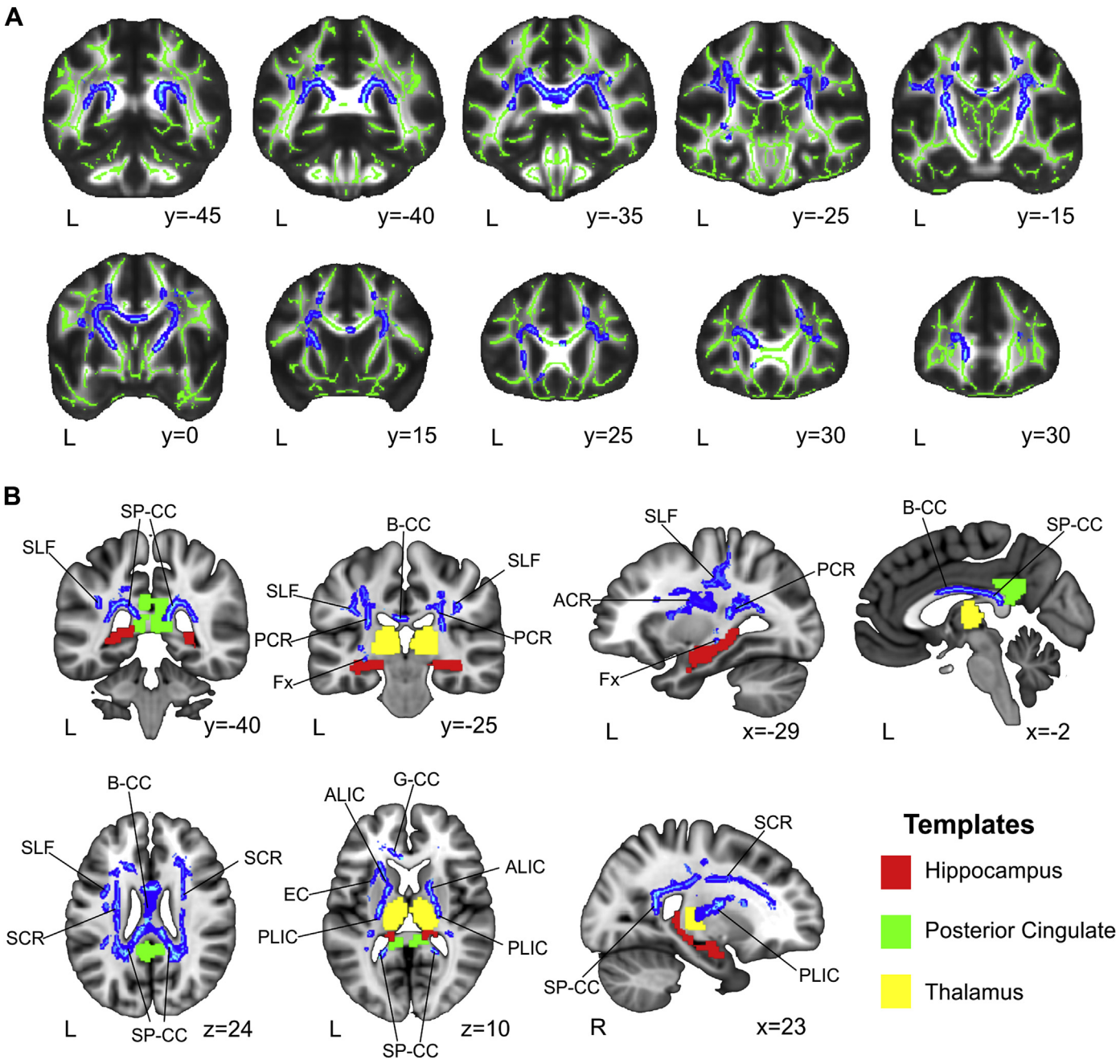

Fig. 1. (A) Tracts showing increased AxD in CN_Aβ42+ compared with CN_Aβ42− (blue) over a mean skeleton (green) and the FMRIB58_FA template, for better visualization of the white matter pathways. (B) Same tracts showing increased AxD in CN_Aβ42+ compared with CN_Aβ42− (blue). In this case, results are displayed on a canonical T1-weighted template for improved localization of the subcortical structures. Templates for the hippocampus (red), posterior cingulate (green), and thalamus (yellow) are also shown. In both cases, results are shown at an FWE-corrected $p < 0.05$ threshold. Neurologic conventions and MNI coordinates are used. Abbreviations: ACR, anterior corona radiata; ALIC, anterior limb of the internal capsule; AxD, axial diffusivity; B-CC, body of the corpus callosum; EC, extreme capsule; Fx, fornix; G-CC, genu of the corpus callosum; L, left hemisphere; PCR, posterior corona radiata; PLIC, posterior limb of the internal capsule; R, right hemisphere; SCR, superior corona radiata; SLF, superior longitudinal fasciculus; SP-CC, splenium of the corpus callosum.

Previous data suggest that DTI indexes can be a sensitive measure for detecting microstructural WM changes in AD, and may be an early indicator of the pathologic process of the disease (Acosta-Cabronero et al., 2010). The study of DTI indexes and their changes over time opens up a new field to explore the temporal and spatial evolution of WM damage at onset of AD and during its evolution. Although FA (a robust DTI index linked to WM integrity) and RD (a DTI measure more related to myelin degradation; Beaulieu, 2002; Fields, 2008; Kim et al., 2006; Song et al., 2002) vary with the progression of the pathology, AxD has been proposed as one of the first DTI indexes to show an early change in AD (Acosta-Cabronero et al., 2012). AxD represents the diffusivity of water parallel to white matter fibers, and its decrease has been directly related to axonal damage or the loss of fiber tracts (Beaulieu, 2002; Loy et al., 2007; Song et al., 2002, 2005). Although experimental studies have demonstrated a link between decreased AxD and axonal damage (Budde et al., 2009; DeBoy et al., 2007), some studies in aging and demented brain

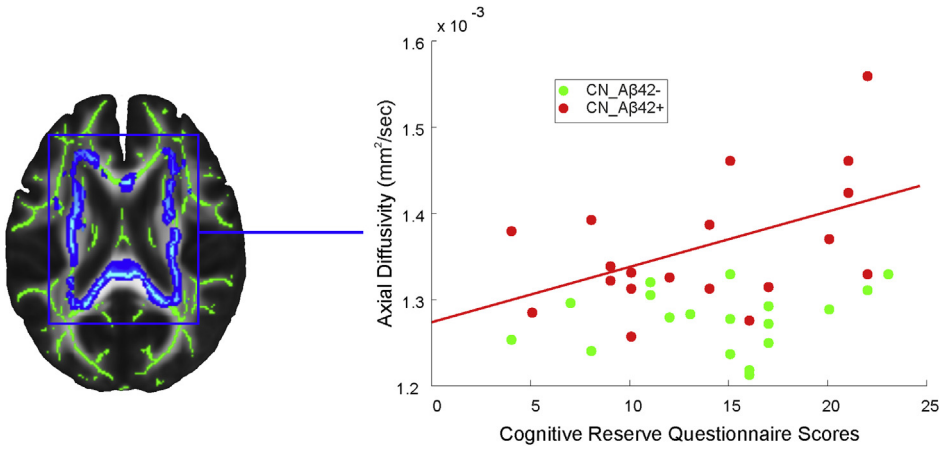

Fig. 2. Scatter plot displaying the relationship between the areas showing increased AxD in CN_Aβ42+ and the scores from the cognitive reserve questionnaire (only significant for the CN_Aβ42+ ($r = 0.57$, $p < 0.013$). Red and green dots are used for the CN_Aβ42+ and CN_Aβ42− groups, respectively. Abbreviation: AxD, axial diffusivity.

have demonstrated both a decrease and an increase in AxD (Acosta-Cabronero et al, 2012; Burzynska et al., 2010). It has been hypothesized that after fiber degeneration, the fragmentation of axons creates barriers to the longitudinal displacement of water molecules, resulting in an initial decrease of AxD. This cellular debris is subsequently cleared by microglia, reestablishing diffusion parallel to the remaining axons that result in an increase in diffusion in the longitudinal direction, thus also increasing Ax-D (Concha et al., 2006; Sun et al., 2008). In this study, CN_Aβ42+ showed increased AxD compared with CN_Aβ42−, although no other DTI measures revealed significant differences between CN_Aβ42+ and CN_Aβ42− groups, suggesting the existence of differentiated white matter microstructures in CN_Aβ42+ potentially linked to subtle WM changes. Increased AxD is a common finding in patients already diagnosed with AD or mild cognitive impairment (Acosta-Cabronero, 2010, 2012; O'Dwyer et al., 2011; Salat et al., 2010) and also in other neurodegenerative disorders such as Huntington disease (Rosas et al., 2010), Gulf War Illness (Rayhan et al., 2013),

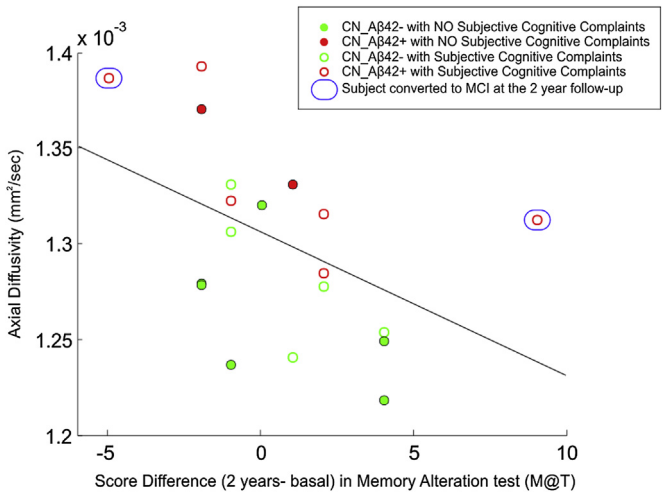

Fig. 3. Relationship between changes (a 2-year follow-up basal) in memory scores (M@T test) and AxD values in the subset of subjects who underwent longitudinal follow-up. CN_Aβ42+ are depicted in red circles (filled for CN_Aβ42+ with no subjective cognitive complaints) and CN_Aβ42− are shown in green circles (filled for CN_Aβ42− subjects with no subjective cognitive complaints). Subjects who converted to MCI at the 2 years follow-up are further marked with a blue ellipse. Abbreviations: AxD, axial diffusivity; MCI, mild cognitive impairment.

Friedreich ataxia (Della Nave et al., 2011) or amyotrophic lateral sclerosis (Metwalli et al., 2010). The pathologic increase in AxD has been related to several potential factors: (1) in areas of crossing white matter tracts, in which the tensor is the average of each tract passing through a particular voxel, the degeneration of one or more of the crossing white matter fibers can yield an increase in AxD, as the tensor will be driven only by the surviving white matter pathways (Acosta-Cabronero et al., 2012; Douaud et al., 2011; O'Dwyer et al., 2011); (2) the activation of microglial cells within an inflammatory process following axonal damage, can contribute to the clearance of axonal fragments, thus, facilitating again the longitudinal diffusion of water molecules and the corresponding increase in AxD (Acosta-Cabronero et al., 2012; O'Dwyer et al., 2011); (3) and finally, axonal atrophy can lead to increased extra-axonal space, which allows water molecules to move faster parallel to the axons, eventually leading to increases in AxD (Della Nave et al., 2011; Rosas et al., 2010). In spite of all these studies, the exact mechanism underlying pathologic AxD increases remains unknown.

To date, amyloid CSF levels have been described as the most sensitive biomarkers at the presymptomatic stage of AD, as changes in this marker (Bateman et al., 2012; Jack et al., 1999) commonly precede brain structural degeneration. Specifically, decreased FA and increased RD values are commonly observed in AD patients at the dementia stage, whereas amyloid deposition is believed to occur 20 years before the clinical onset of the disease (Villemagne et al., 2013). The preservation of FA along with RD may indicate that white matter structure, myelination, and probably axonal diameter (Song et al., 2002) are still widely preserved despite low Aβ42 levels in this presymptomatic stage of AD. Based on our results, we hypothesize that the changes observed in AxD in preclinical patients represent the first steps of WM damage in the AD continuum. Therefore, our findings support the idea that changes in AxD, measured by MRI-DTI scanning, one of the safest and easiest methods for screening potential preclinical populations, are a sensitive biomarker that may help to identify patients at risk of developing AD at a very early stage, even before they present any cognitive decline. Nevertheless, in a longitudinal follow-up exam, we found that subjects with higher AxD levels showed greater memory decline after 2 years. This finding is in agreement with those of Selnes et al. (2013), who found that DTI parameters (FA, RD, and MD) were better predictors of cognitive decline than CSF biomarkers in a population of pre-dementia patients (suffering from subjective cognitive impairment and mild cognitive impairment)

over a 2 to 3-year follow-up. This further supports the idea that DTI measures, in this case, AxD could be an independent predictor of early decline in the hypothetical AD biomarker model. Furthermore, the fact that all converters within the group with low Aβ42 levels were also complainers, suggests that the preclinical AD represents a continuum, from completely asymptomatic biomarker positive individuals to those with subtle decline, which may not be sufficient to cause a neuropsychological deficit but could be associated with subjective symptoms.

In our study, several of the white matter pathways that showed WM abnormalities (including corpus callosum, corona radiata, internal capsule, SLF, fornix, uncinate fasciculus and IFOF) connect subcortical and cortical structures that are involved in the initial stages of the disease, such as the hippocampus and the posterior cingulate cortex. Hypometabolism in the hippocampus, posterior cingulate, and anterior thalamus is a common finding in early AD patients (Jack et al., 1999; Minoshima et al., 1997; Nestor et al., 2003; Pengas et al., 2010) and white matter degeneration of tracts connecting these structures has been shown in later stages of the disease (Acosta-Cabronero et al., 2010). These previously described areas of WM abnormalities coincide with the ones shown in Fig. 1B, where WM tracts connecting the hippocampus, thalamus, and posterior cingulate cortex show increased AxD in the CN_Aβ42+. Our findings of increased AxD in the white matter bundles linking regions related to the default mode network (DMN) such as the posterior cingulum and precuneus corroborate those of a number of studies that have described early damage in these posterior regions in CN_Aβ42+ (Sheline et al., 2010). The posterior cingulum and precuneus are part of an important hub that sustains information transfer between the parahippocampal gyrus and the prefrontal cortex. This network is responsible for sustaining memory function related to the DMN, which has also been shown to be part of a memory system that is deactivated during successful encoding and activated during successful retrieval processes (Daselaar et al., 2004; Vannini et al., 2011). Recently, our group has shown that CN_Aβ42+ had significantly different activation of the precuneus and posterior cingulate cortex, core regions of DMN, using functional MRI during an encoding memory task (Rami et al., 2012). These results are in agreement with other studies reporting subtle functional changes during the resting state in healthy subjects with positive pittsburg compound-B (PIB) (Hedden et al., 2009; Nelissen et al., 2007; Sheline et al., 2010; Sperling et al., 2009). Taken together, these DTI and functional findings affecting the precuneus and posterior cingulate cortex in CN_Aβ42+ point to an association between cerebral amyloidosis in the preclinical stage of AD, and subtle axonal and functional changes in the medial parietal areas suggesting that these cortical hub regions could be particularly vulnerable in the early neurodegenerative process associated with an elevated amyloid burden.

Albeit in our study when we assessed the relationship between Aβ42, t-tau, and p-tau with DTI measures, no strong correlations emerged. This might suggest that AxD and Aβ42 behave as independent biomarkers; future studies are needed to further confirm our results. In that sense, another study found an association between tau protein and DTI measures in healthy younger relatives of AD subjects. Bendlin et al. (2012) showed that CSF t-tau and/or Aβ42 predicted white matter microstructure changes 3.5 years later in healthy middle-aged adults with a parental family history of AD. They found that T-tau and T-tau/AB were widely correlated with indices of brain microstructure (mean, axial, and radial diffusivity), notably in regions close to gray matter structures affected in the earliest stages of AD, particularly in a large swathe of temporal lobe white matter adjacent to the hippocampus.

One of the most important findings of our study was the relation between higher scores in the cognitive reserve questionnaire and greater AxD only for the CN_Aβ42+, suggesting that subjects with higher cognitive reserve tolerate greater WM changes. One possible interpretation of this association could be that although a more advanced biological process triggered by amyloid may already be present in these subjects; their cognitive reserve may work as a buffer, delaying the appearance of the classical cognitive impairments associated with AD. In other words, subjects with higher cognitive reserve have greater coping capacities, presenting normal cognitive functioning despite showing earlier WM alterations such as increased AxD values. These findings are in agreement with results recently reported by our group in a similar population, which presented the same type of CR relation but with gray matter changes (Arenaza-Urquijo et al., 2013). Our group found a significant relationship between decreased volumes of the left hippocampus or decreased cortical thickness of the right supramarginal gyrus and higher cognitive reserve scores in a similar CN_Aβ42+. Overall, it seems that subjects with CN_Aβ42+ and higher scores on cognitive reserve questionnaires may tolerate a greater loss of gray matter in critical cortical and subcortical regions together with earlier WM changes. The present results emphasize the importance of evaluating cognitive reserve and of using neuroimaging techniques for early diagnosis in individuals with higher reserve.

Results derived from this study are subject to some limitations that have to be taken into account. The main limitation of this study is its cross-sectional nature. Future longitudinal studies are needed to define DTI-structural and cognitive changes in this CN_Aβ42+. Finally, another limitation is associated to the current CN_Aβ42+ definition. Although we found subtle cognitive changes in naming in a subgroup of 8 CN_Aβ42+ and 5 subjects actually developed MCI because of AD, it is not currently known whether or what proportion of these subjects will finally develop clinical AD and do in fact have preclinical AD; this will only be determined by longitudinal follow-up over a long period of time.

In summary, our results suggest that AxD abnormalities can be detected through DTI-MR measures in the preclinical stage of AD, indicating that subtle white matter changes may precede other biomarkers across the AD continuum. In addition, cognitive reserve seems to modulate the clinical expression of these early WM changes, preserving cognitive functioning in patients with more advanced structural damage. The preservation of other DTI indexes in early stages of the disease continuum may indicate that AxD could serve as an early biomarker of AD preclinical disease.

Disclosure statement

José Luis Molinuevo has provided scientific advice or has been an investigator or data monitoring board member receiving consultancy fees from Pfizer, Eisai, Janssen-Cilag, Novartis, Lundbeck, Roche, Bayer, Bristol-Myers Squibb, GE Health Care, GlaxoSmithKline, Merz, MSD, Avid, Lilly, Biokit and Fujireibio-Europe. The rest of the authors have no current or potential conflicts of interest.

Acknowledgements

The authors thank all the volunteers for participating in this study. This work was supported by Spanish Ministry of Science. Dr Lorena Rami is the recipient of a Miguel Servet grant as a senior investigator from the Spanish Ministry of Science (CP08/00147). This study was funded by research grants from the Spanish *Ministerio de Ciencia e Innovación* to Dr Lorena Rami (FIS PI11/01071), Fondo europeo de desarrollo regional, una manera de hacer Europa,

grant from IMSERSO 197/2011 to Dr Molinuevo (CONSOLIDER grant 2010-00045 and to the Innovative Medicines Initiative Joint Undertaking under grant agreement n°115568, resources of which are composed of financial contribution from the European Union's Seventh Framework Programme (FP7/2007–2013) and EFPIA companies' in kind contribution to Dr Lladó (PI11/00234), P. Ripollés (FPU AP2010-4179), and to Dr Rodríguez-Fornells (PSI2011-29219 and Generalitat de Catalunya grant 2009 SGR 93).

Appendix A. Supplementary data

Supplementary data associated with this article can be found, in the online version, at http://dx.doi.org/10.1016/j.neurobiolaging.2014.05.027.

References

Acosta-Cabronero, J., Williams, G.B., Pengas, G., Nestor, P.J., 2010. Absolute diffusivities define the landscape of white matter degeneration in Alzheimer's disease. Brain 133, 529–539.

Acosta-Cabronero, J., Alley, S., Williams, G.B., Pengas, G., Nestor, P.J., 2012. Diffusion tensor metrics as biomarkers in Alzheimer's disease. PLoS One 7, e49072.

Alexander, A.L., Lee, J.E., Lazar, M., Field, A.S., 2007. Diffusion tensor imaging of the brain. Neurotherapeutics 4, 316–329.

Andersson, J.L.R., Jenkinson, M., Smith, S.M., 2007a. Non-linear optimisation. FMRIB Tech. Rep. TR07JA1. Available at: www.fmrib.ox.ac.uk/analysis/techrep.

Andersson, J.L.R., Jenkinson, M., Smith, S.M., 2007b. Non-linear registration, aka spatial normalisation. FMRIB Tech. Rep. TR07JA2. Available at: www.fmrib.ox.ac.uk/analysis/techrep.

Antonell, A., Fortea, J., Rami, L., Bosch, B., Balasa, M., Sánchez-Valle, R., Iranzo, A., Molinuevo, J.L., Lladó, A., 2011. Different profiles of Alzheimer's disease cerebrospinal fluid biomarkers in controls and subjects with subjective memory complaints. J. Neural Transm. 118, 259–262.

Arenaza-Urquijo, E.M., Molinuevo, J.L., Sala-Llonch, R., Sole-Padulles, C., Balasa, M., Bosch, B., Olives, J., Antonell, A., Llado, A., Sanchez-Valle, R., Rami, L., Bartres-Faz, D., 2013. Cognitive reserve proxies relate to gray matter loss in cognitively healthy elderly with abnormal cerebrospinal fluid amyloid-beta levels. J. Alzheimers. Dis. 35, 715–726.

Basser, P.J., Mattiello, J., LeBihan, D., 1994a. Estimation of the effective self-diffusion tensor from the NMR spin echo. J. Magn. Reson. B. 103, 247–254.

Basser, P.J., Mattiello, J., LeBihan, D., 1994b. MR diffusion tensor spectroscopy and imaging. Biophys. J. 66, 259–267.

Bateman, R.J., Xiong, C., Benzinger, T.L., Fagan, A.M., Goate, A., Fox, N.C., Marcus, D.S., Cairns, N.J., Xie, X., Blazey, T.M., Holtzman, D.M., Santacruz, A., Buckles, V., Oliver, A., Moulder, K., Aisen, P.S., Ghetti, B., Klunk, W.E., McDade, E., Martins, R.N., Masters, C.L., Mayeux, R., Ringman, J.M., Rossor, M.N., Schofield, P.R., Sperling, R.A., Salloway, S., Morris, J.C., 2012. Clinical and biomarker changes in dominantly inherited Alzheimer's disease. N. Engl. J. Med. 367, 795–804.

Beaulieu, C., 2002. The basis of anisotropic water diffusion in the nervous system - a technical review. NMR Biomed. 15, 435–455.

Bendlin, B.B., Carlsson, C.M., Johnson, S.C., Zetterberg, H., Blennow, K., Willette, A.A., Okonkwo, O.C., Sodhi, A., Ries, M.L., Birdsill, A.C., Alexander, A.L., Rowley, H.A., Puglielli, L., Asthana, S., Sager, M.A., 2012. CSF T-Tau/Abeta42 predicts white matter microstructure in healthy adults at risk for Alzheimer's disease. PLoS One 7, e37720.

Bosch, B., Arenaza-Urquijo, E.M., Rami, L., Sala-Llonch, R., Junque, C., Sole-Padulles, C., Pena-Gomez, C., Bargallo, N., Molinuevo, J.L., Bartres-Faz, D., 2012. Multiple DTI index analysis in normal aging, amnestic MCI and AD. Relationship with neuropsychological performance. Neurobiol. Aging 33, 61–74.

Budde, M.D., Xie, M., Cross, A.H., Song, S.K., 2009. Axial diffusivity is the primary correlate of axonal injury in the experimental autoimmune encephalomyelitis spinal cord: a quantitative pixelwise analysis. J. Neurosci. 29, 2805–2813.

Burzynska, A.Z., Preuschhof, C., Bäckman, L., Nyberg, L., Li, S.C., Lindenberger, U., Heekeren, H.R., 2010. Age-related differences in white matter microstructure: region-specific patterns of diffusivity. Neuroimage 49, 2104–2112.

Concha, L., Gross, D.W., Wheatley, B.M., Beaulieu, C., 2006. Diffusion tensor imaging of time-dependent axonal and myelin degradation after corpus callosotomy in epilepsy patients. Neuroimage 32, 1090–1099.

Daselaar, S.M., Prince, S.E., Cabeza, R., 2004. When less means more: deactivations during encoding that predict subsequent memory. Neuroimage 23, 921–927.

DeBoy, C.A., Zhang, J., Dike, S., Shats, I., Jones, M., Reich, D.S., Mori, S., Nguyen, T., Rothstein, B., Miller, R.H., Griffin, J.T., Kerr, D.A., Calabresi, P.A., 2007. High resolution diffusion tensor imaging of axonal damage in focal inflammatory and demyelinating lesions in rat spinal cord. Brain 130, 2199–2210.

Della Nave, N.R., Ginestroni, A., Diciotti, S., Salvatore, E., Soricelli, A., Mascalchi, M., 2011. Axial diffusivity is increased in the degenerating superior cerebellar peduncles of Friedreich's ataxia. Neuroradiology 53, 367–372.

Douaud, G., Jbabdi, S., Behrens, T.E., Menke, R.A., Gass, A., Monsch, A.U., Rao, A., Whitcher, B., Kindlmann, G., Matthews, P.M., Smith, S., 2011. DTI measures in crossing-fibre areas: increased diffusion anisotropy reveals early white matter alteration in MCI and mild Alzheimer's disease. Neuroimage 55, 880–890.

Dubois, B., Feldman, H.H., Jacova, C., Cummings, J.L., Dekosky, S.T., Barberger-Gateau, P., Delacourte, A., Frisoni, G., Fox, N.C., Galasko, D., Gauthier, S., Hampel, H., Jicha, G.A., Meguro, K., O'Brien, J., Pasquier, F., Robert, P., Rossor, M., Salloway, S., Sarazin, M., de Souza, L.C., Stern, Y., Visser, P.J., Scheltens, P., 2010. Revising the definition of Alzheimer's disease: a new lexicon. Lancet Neurol. 9, 1118–1127.

Fellgiebel, A., Muller, M.J., Wille, P., Dellani, P.R., Scheurich, A., Schmidt, L.G., Stoeter, P., 2005. Color-coded diffusion-tensor-imaging of posterior cingulate fiber tracts in mild cognitive impairment. Neurobiol. Aging 26, 1193–1198.

Fields, R.D., 2008. White matter in learning, cognition and psychiatric disorders. Trends. Neurosci. 31, 361–370.

Fortea, J., Sala-Llonch, R., Bartres-Faz, D., Llado, A., Sole-Padulles, C., Bosch, B., Antonell, A., Olives, J., Sanchez-Valle, R., Molinuevo, J.L., Rami, L., 2011. Cognitively preserved subjects with transitional cerebrospinal fluid ss-amyloid 1-42 values have thicker cortex in Alzheimer's disease vulnerable areas. Biol. Psychiatry 70, 183–190.

Hedden, T., Van Dijk, K.R., Becker, J.A., Mehta, A., Sperling, R.A., Johnson, K.A., Buckner, R.L., 2009. Disruption of functional connectivity in clinically normal older adults harboring amyloid burden. J. Neurosci. 29, 12686–12694.

Iacono, D., O'Brien, R., Resnick, S.M., Zonderman, A.B., Pletnikova, O., Rudow, G., An, Y., West, M.J., Crain, B., Troncoso, J.C., 2008. Neuronal hypertrophy in asymptomatic Alzheimer disease. J. Neuropathol. Exp. Neurol. 67, 578–589.

Jack Jr., C.R., Petersen, R.C., Xu, Y.C., O'Brien, P.C., Smith, G.E., Ivnik, R.J., Boeve, B.F., Waring, S.C., Tangalos, E.G., Kokmen, E., 1999. Prediction of AD with MRI-based hippocampal volume in mild cognitive impairment. Neurology 52, 1397–1403.

Jack Jr., C.R., Knopman, D.S., Jagust, W.J., Shaw, L.M., Aisen, P.S., Weiner, M.W., Petersen, R.C., Trojanowski, J.Q., 2010. Hypothetical model of dynamic biomarkers of the Alzheimer's pathological cascade. Lancet Neurol. 9, 119–128.

Jenkinson, M., Smith, S., 2001. A global optimisation method for robust affine registration of brain images. Med. Image Anal. 5, 143–156.

Jenkinson, M., Beckmann, C.F., Behrens, T.E., Woolrich, M.W., Smith, S.M., 2012. FSL. Neuroimage 62, 782–790.

Kalus, P., Slotboom, J., Gallinat, J., Mahlberg, R., Cattapan-Ludewig, K., Wiest, R., 2006. Examining the gateway to the limbic system with diffusion tensor imaging: the perforant pathway in dementia. Neuroimage 30, 713–720.

Katzman, R., 1993. Education and the prevalence of dementia and Alzheimer's disease. Neurology 43, 13–20.

Kim, J.H., Budde, M.D., Liang, H.F., Klein, R.S., Russell, J.H., Cross, A.H., Song, S.K., 2006. Detecting axon damage in spinal cord from a mouse model of multiple sclerosis. Neurobiol. Dis. 21, 626–632.

Leemans, A., Jones, D.K., 2009. The B-matrix must be rotated when correcting for subject motion in DTI data. Magn. Reson. Med. 61, 1336–1349.

Loy, D.N., Kim, J.H., Xie, M., Schmidt, R.E., Trinkaus, K., Song, S.K., 2007. Diffusion tensor imaging predicts hyperacute spinal cord injury severity. J. Neurotrauma 24, 979–990.

Maldjian, J.A., Laurienti, P.J., Kraft, R.A., Burdette, J.H., 2003. An automated method for neuroanatomic and cytoarchitectonic atlas-based interrogation of fMRI data sets. Neuroimage 19, 1233–1239.

Maldjian, J.A., Laurienti, P.J., Burdette, J.H., 2004. Precentral gyrus discrepancy in electronic versions of the Talairach atlas. Neuroimage 21, 450–455.

Medina, D., DeToledo-Morrell, L., Urresta, F., Gabrieli, J.D., Moseley, M., Fleischman, D., Bennett, D.A., Leurgans, S., Turner, D.A., Stebbins, G.T., 2006. White matter changes in mild cognitive impairment and AD: a diffusion tensor imaging study. Neurobiol. Aging 27, 663–672.

Metwalli, N.S., Benatar, M., Nair, G., Usher, S., Hu, X., Carew, J.D., 2010. Utility of axial and radial diffusivity from diffusion tensor MRI as markers of neurodegeneration in amyotrophic lateral sclerosis. Brain Res. 1348, 156–164.

Minoshima, S., Giordani, B., Berent, S., Frey, K.A., Foster, N.L., Kuhl, D.E., 1997. Metabolic reduction in the posterior cingulate cortex in very early Alzheimer's disease. Ann. Neurol. 42, 85–94.

Nelissen, N., Vandenbulcke, M., Fannes, K., Verbruggen, A., Peeters, R., Dupont, P., Van Laere, K., Bormans, G., Vandenberghe, R., 2007. Abeta amyloid deposition in the language system and how the brain responds. Brain 130, 2055–2069.

Nestor, P.J., Fryer, T.D., Smielewski, P., Hodges, J.R., 2003. Limbic hypometabolism in Alzheimer's disease and mild cognitive impairment. Ann. Neurol. 54, 343–351.

Nichols, T.E., Holmes, A.P., 2002. Nonparametric permutation tests for functional neuroimaging: a primer with examples. Hum. Brain Mapp. 15, 1–25.

O'Dwyer, L., Lamberton, F., Bokde, A.L., Ewers, M., Faluyi, Y.O., Tanner, C., Mazoyer, B., O'Neill, D., Bartley, M., Collins, D.R., Coughlan, T., Prvulovic, D., Hampel, H., 2011. Multiple indices of diffusion identifies white matter damage in mild cognitive impairment and Alzheimer's disease. PLoS One 6, e21745.

Pengas, G., Hodges, J.R., Watson, P., Nestor, P.J., 2010. Focal posterior cingulate atrophy in incipient Alzheimer's disease. Neurobiol. Aging 31, 25–33.

Rami, L., Gómez-Ansón, B., Bosch, B., Sánchez-Valle, R., Monte, G.C., Villar, A., Molinuevo, J.L., 2007. Cortical brain metabolism as measured by proton spectroscopy is related to memory performance in patients with amnestic mild cognitive impairment and Alzheimer's disease. Dement. Geriatr. Cogn. Disord. 24, 274–279.

Rami, L., Valls-Pedret, C., Bartrés-Faz, D., Caprile, C., Solé-Padullés, C., Castellvi, M., Olives, J., Bosch, B., Molinuevo, J.L., 2011. Cognitive reserve questionnaire. Scores obtained in a healthy elderly population and in one with Alzheimer's disease. Rev. Neurol. 52, 195–201.

Rami, L., Sala-Llonch, R., Sole-Padulles, C., Fortea, J., Olives, J., Llado, A., Pena-Gomez, C., Balasa, M., Bosch, B., Antonell, A., Sanchez-Valle, R., Bartres-Faz, D., Molinuevo, J.L., 2012. Distinct functional activity of the precuneus and posterior cingulate cortex during encoding in the preclinical stage of Alzheimer's disease. J. Alzheimers. Dis. 31, 517–526.

Rayhan, R.U., Stevens, B.W., Timbol, C.R., Adewuyi, O., Walitt, B., VanMeter, J.W., Baraniuk, J.N., 2013. Increased brain white matter axial diffusivity associated with fatigue, pain and hyperalgesia in Gulf War Illness. PLoS One 8, e58493.

Ripolles, P., Marco-Pallares, J., de Diego-Balaguer, R., Miro, J., Falip, M., Juncadella, M., Rubio, F., Rodriguez-Fornells, A., 2012. Analysis of automated methods for spatial normalization of lesioned brains. Neuroimage 60, 1296–1306.

Rosas, H.D., Lee, S.Y., Bender, A.C., Zaleta, A.K., Vangel, M., Yu, P., Fischl, B., Pappu, V., Onorato, C., Cha, J.H., Salat, D.H., Hersch, S.M., 2010. Altered white matter microstructure in the corpus callosum in Huntington's disease: implications for cortical "disconnection". Neuroimage 49, 2995–3004.

Ryan, N.S., Keihaninejad, S., Shakespeare, T.J., Lehmann, M., Crutch, S.J., Malone, I.B., Thornton, J.S., Mancini, L., Hyare, H., Yousry, T., Ridgway, G.R., Zhang, H., Modat, M., Alexander, D.C., Rossor, M.N., Ourselin, S., Fox, N.C., 2013. Magnetic resonance imaging evidence for presymptomatic change in thalamus and caudate in familial Alzheimer's disease. Brain 136, 1399–1414.

Salat, D.H., Tuch, D.S., van der Kouwe, A.J., Greve, D.N., Pappu, V., Lee, S.Y., Hevelone, N.D., Zaleta, A.K., Growdon, J.H., Corkin, S., Fischl, B., Rosas, H.D., 2010. White matter pathology isolates the hippocampal formation in Alzheimer's disease. Neurobiol. Aging 31, 244–256.

Selnes, P., Aarsland, D., Bjornerud, A., Gjerstad, L., Wallin, A., Hessen, E., Reinvang, I., Grambaite, R., Auning, E., Kjaervik, V.K., Due-Tonnessen, P., Stenset, V., Fladby, T., 2013. Diffusion tensor imaging surpasses cerebrospinal fluid as predictor of cognitive decline and medial temporal lobe atrophy in subjective cognitive impairment and mild cognitive impairment. J. Alzheimers. Dis. 33, 723–736.

Sheline, Y.I., Raichle, M.E., Snyder, A.Z., Morris, J.C., Head, D., Wang, S., Mintun, M.A., 2010. Amyloid plaques disrupt resting state default mode network connectivity in cognitively normal elderly. Biol. Psychiatry 67, 584–587.

Smith, S.M., 2002. Fast robust automated brain extraction. Hum. Brain Mapp. 17, 143–155.

Smith, S.M., Nichols, T.E., 2009. Threshold-free cluster enhancement: addressing problems of smoothing, threshold dependence and localisation in cluster inference. Neuroimage 44, 83–98.

Smith, S.M., Jenkinson, M., Woolrich, M.W., Beckmann, C.F., Behrens, T.E., Johansen-Berg, H., Bannister, P.R., De, L.M., Drobnjak, I., Flitney, D.E., Niazy, R.K., Saunders, J., Vickers, J., Zhang, Y., De, S.N., Brady, J.M., Matthews, P.M., 2004. Advances in functional and structural MR image analysis and implementation as FSL. Neuroimage 23 (Suppl. 1), S208–S219.

Smith, S.M., Jenkinson, M., Johansen-Berg, H., Rueckert, D., Nichols, T.E., Mackay, C.E., Watkins, K.E., Ciccarelli, O., Cader, M.Z., Matthews, P.M., Behrens, T.E., 2006. Tract-based spatial statistics: voxelwise analysis of multi-subject diffusion data. Neuroimage 31, 1487–1505.

Song, S.K., Sun, S.W., Ramsbottom, M.J., Chang, C., Russell, J., Cross, A.H., 2002. Dysmyelination revealed through MRI as increased radial (but unchanged axial) diffusion of water. Neuroimage 17, 1429–1436.

Song, S.K., Yoshino, J., Le, T.Q., Lin, S.J., Sun, S.W., Cross, A.H., Armstrong, R.C., 2005. Demyelination increases radial diffusivity in corpus callosum of mouse brain. Neuroimage 26, 132–140.

Sperling, R.A., Laviolette, P.S., O'Keefe, K., O'Brien, J., Rentz, D.M., Pihlajamaki, M., Marshall, G., Hyman, B.T., Selkoe, D.J., Hedden, T., Buckner, R.L., Becker, J.A., Johnson, K.A., 2009. Amyloid deposition is associated with impaired default network function in older persons without dementia. Neuron 63, 178–188.

Sperling, R.A., Aisen, P.S., Beckett, L.A., Bennett, D.A., Craft, S., Fagan, A.M., Iwatsubo, T., Jack Jr., C.R., Kaye, J., Montine, T.J., Park, D.C., Reiman, E.M., Rowe, C.C., Siemers, E., Stern, Y., Yaffe, K., Carrillo, M.C., Thies, B., Morrison-Bogorad, M., Wagster, M.V., Phelps, C.H., 2011. Toward defining the preclinical stages of Alzheimer's disease: recommendations from the National Institute on Aging-Alzheimer's Association workgroups on diagnostic guidelines for Alzheimer's disease. Alzheimers Dement. 7, 280–292.

Stern, Y., 2009. Cognitive reserve. Neuropsychologia 47, 2015–2028.

Sun, S.W., Liang, H.F., Cross, A.H., Song, S.K., 2008. Evolving Wallerian degeneration after transient retinal ischemia in mice characterized by diffusion tensor imaging. Neuroimage 40, 1–10.

Vannini, P., O'Brien, J., O'Keefe, K., Pihlajamäki, M., Laviolette, P., Sperling, R.A., 2011. What goes down must come up: role of the posteromedial cortices in encoding and retrieval. Cereb. Cortex 21, 22–34.

Villemagne, V.L., Burnham, S., Bourgeat, P., Brown, B., Ellis, K.A., Salvado, O., Szoeke, C., Macaulay, S.L., Martins, R., Maruff, P., Ames, D., Rowe, C.C., Masters, C.L., 2013. Amyloid β deposition, neurodegeneration, and cognitive decline in sporadic Alzheimer's disease: a prospective cohort study. Lancet Neurol. 12, 357–367.

Wahlund, L.O., Barkhof, F., Fazekas, F., Bronge, L., Augustin, M., Sjogren, M., Wallin, A., Ader, H., Leys, D., Pantoni, L., Pasquier, F., Erkinjuntti, T., Scheltens, P., 2001. A new rating scale for age-related white matter changes applicable to MRI and CT. Stroke 32, 1318–1322.

Woolrich, M.W., Jbabdi, S., Patenaude, B., Chappell, M., Makni, S., Behrens, T., Beckmann, C., Jenkinson, M., Smith, S.M., 2009. Bayesian analysis of neuroimaging data in FSL. Neuroimage 45, S173–S186.